Journal of Nuclear Materials 384 (2009) 303–310

Contents lists available at ScienceDirect

Journal of Nuclear Materials

journal homepage: www.elsevier.com/locate/jnucmat

Characterization of $(Th,U)O_2$ pellets made by advanced CAP process

T.R.G. Kutty [a,*], P.S. Somayajulu [b], K.B. Khan [a], Arun Kumar [a], H.S. Kamath [c]

[a] Radiometallurgy Division, Bhabha Atomic Research Centre, Mumbai 400 085, India
[b] Advanced Fuel Fabrication Facility, Tarapur, India
[c] Nuclear Fuels Group, Bhabha Atomic Research Centre, Mumbai 400 085, India

ARTICLE INFO

Article history:
Received 16 June 2008
Accepted 3 December 2008

PACS:
61.72
81.20.Ev
62.20. Fe
81.70.P

ABSTRACT

Coated Agglomerate Pelletization (CAP) process is being developed by Bhabha Atomic Research Centre (BARC) for the fabrication of ThO_2–UO_2 mixed oxide fuel pellets. In order to improve the microstructures with better microhomogeneity, a study was made to modify the CAP process. The advanced CAP (A-CAP) process is similar to the CAP process except that the co-precipitated powder of mixed oxide, ThO_2–30%UO_2 or ThO_2–50%UO_2, is used for coating instead of U_3O_8 powder. The choice of ThO_2–UO_2 powders as the coating material is advantageous compared to U_3O_8, since the presence of large quantities of ThO_2 in UO_2 powder gives better self-shielding effect. In this paper, ThO_2 containing 4%UO_2 (% in weight) was prepared by the A-CAP process. Property measurements including microstructure and microhomogeneity were made by optical microscopy, scanning electron microscopy (SEM), electron probe microanalysis (EPMA), etc. It was found that the pellets sintered in air at 1400 °C showed a duplex grain structure and those sintered in Ar–8%H_2 at 1650 °C showed a very uniform grain structure with excellent microhomogeneity.

1. Introduction

Recently, a new fabrication procedure using Coated Agglomerate Pelletization (CAP) was developed by Bhabha Atomic Research Centre (BARC) for the fabrication of ThO_2–$^{233}UO_2$ pellets [1,2]. This process is developed to replace the conventional powder metallurgy process that consists of direct blending of $^{233}UO_2$ and ThO_2 powders [3]. There is a difficulty in fabricating the $(Th,^{233}U)O_2$ fuel pellet because ^{233}U is usually accompanied by the daughters of ^{232}U (half-life 69.85 y) namely, ^{212}Bi and ^{208}Tl, which emit strong gamma radiations of 1.62 MeV and 0.511–2.614 MeV, respectively [4]. Therefore, the fabrication of the thorium fuel requires operations in the shielded glove-boxes to protect the operators from radiation [3,5–8]. The radiation exposure problem can also be remedied if the processing of ^{233}U into fuel is quickly finished after the chemical separation of uranium since the half-life of coexisting ^{232}U is much longer than its radioactive daughters. The flow-sheet of the CAP technique is made of the segmented processes to be performed in the unshielded and shielded facilities on the assumption to use freshly prepared ^{233}U oxide in order to minimize man–rem problem. The main reasons for developing the CAP technique to produce $(Th,U)O_2$ fuel are [3]:

- to minimize the dusty operations;
- to minimize the number of process steps requiring shielded operation;
- to reduce the man–rem problems since the use of the highly radioactive ^{233}U (accompanied by ^{232}U) is confined to only certain steps in the fabrication route.

In the CAP process, ThO_2 is converted to free flowing agglomerates by powder extrusion method. As only ThO_2 is handled to this stage, all the operations are carried out in a normal glove-box facility. The subsequent operations are carried out in a shielded glove-box or hot cell facility using manipulators. For the fabrication of ThO_2–4%UO_2 pellets (4 g UO_2 in 96 g ThO_2) using the CAP process, ThO_2 granules and U_3O_8 powders were used as the starting materials. It was found that the ThO_2–4%UO_2 pellets developed by the CAP process showed a 'rock in sand' structure with small grains in the center of the granules and large grains along the periphery [1,2]. However, no delineation of granules could be found. Also it was noticed from the EPMA data that the uranium concentration was slightly higher in the large grained areas. In order to improve the microstructures with better microhomogeneity, the modification of the CAP process was studied. This advanced CAP (A-CAP) is similar to CAP process except that instead of U_3O_8 powder, $(Th,U)O_2$ powders are used for coating. The choice of ThO_2–UO_2 powders as the coating material is advantageous compared to U_3O_8, since the presence of large quantities of ThO_2 in $^{233}UO_2$ powder gives better self-shielding effect. Studies using Monte Carlo

* Corresponding author. Tel.: +91 22 25595361; fax: +91 22 25505151.
E-mail address: tkutty@barc.gov.in (T.R.G. Kutty).

0022-3115/$ - see front matter © 2008 Elsevier B.V. All rights reserved.
doi:10.1016/j.jnucmat.2008.12.038

technique have shown that on mixing $^{233}UO_2$ powder with 50%ThO_2, the dose has come down by about 30%. Therefore, better protection for workers is ensured while manufacturing ThO_2–UO_2 pellets using A-CAP process. $(Th,U)O_2$ powders for the above process were made by the co-precipitation technique.

The goal of this work is to develop mixed thorium–uranium dioxide (ThO_2–UO_2) fuel by advanced CAP technique using ThO_2 granules and $(Th,U)O_2$ powders as the starting material. The mixed oxide fuel is generally manufactured under a stringent quality assurance programme. At each step of the fabrication process, quality assurance plans have been established to verify various factors that affect the fuel performance in the reactor [1]. The criteria for adoption of manufacturing process include the acceptable microstructure and the uniform distribution of fissile elements in the pellet matrix [9,10]. The use of U_3O_8 in the CAP process naturally leads to a consequence that the uranium concentration in the solid solution is higher in the larger grained areas. In an earlier study [2], the authors argued that this concentration inhomogeneity is desirable for fuel because a larger amount of heat is generated at the periphery of the particles. If the designer prefers a process that can deliver pellets having improved microstructures with better microhomogeneity, it is worth to modify the CAP process. A-CAP process can deliver pellets having microstructure which are either similar to CAP process or with the improved ones by selecting the appropriate sintering atmospheres. This paper deals with the procedures for the fabrication of ThO_2–4%UO_2 pellets by A-CAP process and their characterization including optical microscopy, scanning electron microscopy (SEM) and electron probe microanalysis (EPMA).

2. A-CAP process

The flow-sheet of fabrication of $(Th,U)O_2$ pellets by A-CAP process is given in Fig. 1. For A-CAP process, ThO_2 should be in the form of free flowing agglomerate which can be obtained either by pre-compaction and granulation technique or by extrusion of powders. To make free flowing agglomerates by the extrusion route, the ThO_2 powder is mixed with an organic binder (polyethylene glycol) and extruded through perforated rollers. The extruded ThO_2 paste is converted to agglomerates in a spherodiser. The agglomerates are sieved and subsequently dried to remove the organic binder. Earlier study [1] has shown that −40 mesh ThO_2 granules are the best for attaining good microstructure, and therefore the present study was carried out using the above sized granules. As only ThO_2 is handled up to this stage, all these operations are carried out in a normal alpha tight glove-box facility (Fig. 1, upper half). The operations carried out under shielding are (Fig. 1, lower half) [1,3]:

(a) coating of ThO_2 agglomerates with desired amount of ThO_2–UO_2 powders;
(b) compaction in a multi-station rotary press into green pellets;
(c) sintering in air/Ar–H_2;
(d) pellet loading and encapsulation into fuel rods.

The $(Th,U)O_2$ powders used for coating were prepared by using the co-precipitation technique. In this study, ThO_2–30%UO_2 and ThO_2–50%UO_2 powders are prepared (Fig. 1). ThO_2–30%UO_2 is the candidate fuel for the breeder reactor. The higher compositions are chosen so that one can dilute them to any required composition by the addition of ThO_2. As shown in Fig. 2, the procedures for the fabrication of the above powders consist of:

(a) preparation uranyl and thorium nitrate solutions;
(b) reduction of U ions from (VI) to (IV) valency state;
(c) mixing of the solutions to the intended U to Th ratio;
(d) co-precipitation using oxalic acid;
(e) Calcination in air at 700 °C for 3 h.

The details of the preparation of $(Th,U)O_2$ powders by co-precipitation process have been given elsewhere [11].

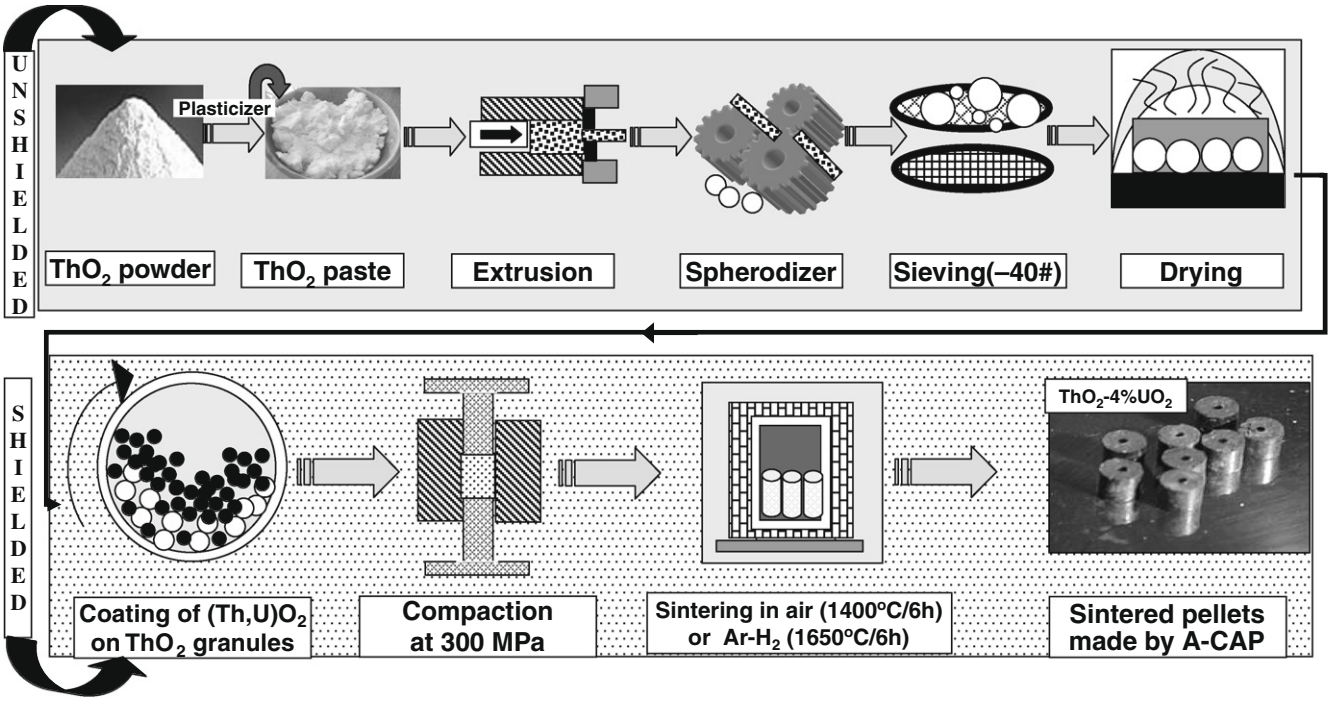

Fig. 1. Schematic diagram of the A-CAP process for the fabrication of $(Th,^{233}U)O_2$ pellets.

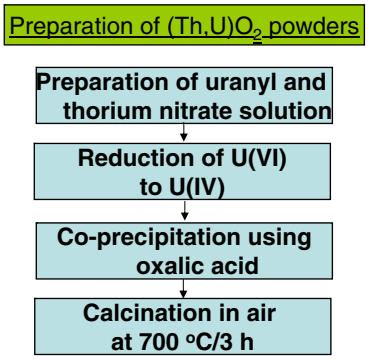

Fig. 2. Flow-sheet for the fabrication of (Th,^{233}U)O_2 pellets by A-CAP process.

3. Experimental

3.1. Preparation of green compacts

The green pellets of ThO_2–4%UO_2 for this study were prepared as described above by the A-CAP process using ThO_2 granules (−40 mesh). In this study, ThO_2–30%UO_2 and ThO_2–50%UO_2 (% in weight) powders are used for coating the above mentioned granules. This work was simulated using natural U instead of ^{233}U. Table 1 gives the typical impurity contents of co-precipitated (Th,U)O_2 powders. The procedure for the fabrication of ThO_2–4%UO_2 green pellets consists of the following steps:

(a) mixing the ThO_2 granules with the required quantity of ThO_2–30%UO_2 or ThO_2–50%UO_2 powders in a planetary ball for 4 h with tungsten carbide balls,
(b) cold compaction of the mixed powder at 300 MPa into green pellets,
(c) Sintering in reducing or oxidizing atmosphere.

The green density of the compacts was in the range of 63–67% of the theoretical density. To facilitate compaction and to impart handling strength to the green pellets, 1 wt% zinc phenate was added as lubricant/binder during the last 1 h of the mixing/milling procedure. The green pellets were 12.1 mm in diameter and around 10 mm in length. The sintering of the ThO_2–4%UO_2 pellets made by A-CAP process was carried out in air at 1400 °C for 6 h. Since diffusion is largely dependent on the oxygen potential of the sintering atmosphere, a few green pellets were sintered separately in Ar–8%H_2 at 1650 °C for 6 h.

3.2. Characterization

The ThO_2–4% UO_2 pellets fabricated by A-CAP process were characterized by means of thermogravimetry, XRD, density measurement, metallography, SEM and EPMA. The O/M ratio of the sintered pellet was measured thermogravimetrically using Bahr (Model STA-503) thermal analyzer. The accuracy of the measurement in weight was ±1 μg. The phase analysis of the ThO_2–UO_2 pellet was carried out by X-ray diffractometry (Diano, Model XRD-8760). The X-ray diffraction patterns of the pellets were obtained by using CuK_α radiation monochromatized by curved graphite monochromator. The minimum detectable limit of this equipment is ±5%. The sintered density was determined by means of the Archimedes method by using ethylene dibromide. For metallography, the sintered pellet was fixed by Araldite and ground using successive grades of emery papers. The final polishing was done by diamond paste. The pellet was removed from the mount by dissolving Araldite with acetone and then etched thermally. The grain size was determined by the intercept method with the help of an optical microscope (Leica make, Model: Polyvar). The microstructure was then characterized by SEM (Philips make, Model: XL-30). The distribution of Th, U and O was determined by X-ray mapping and also by line scans with the help of EPMA (Cameca, Model Sx-100).

Table 1
Impurity contents of (Th,U)O_2 powders made by co-precipitation.

Impurity	ThO_2–50%UO_2 (ppm)	ThO_2–30%UO_2 (ppm)
B	0.1	0.3
Cd	<0.1	<0.1
Co	<5	<5
Ca	<5	<5
Fe	<10	<10
Si	<40	<40
Al	43.4	36.8
Mn	<2	<2
W	<40	<40
Cr	<5	<5
Pb	9.1	12.5

4. Results

The average particle size of the ThO_2–30%UO_2 and ThO_2–50%UO_2 powders used in this study were 0.63±0.21 and 0.81±0.17 μm, respectively. It may be noted that about 90% particles for ThO_2–30%UO_2 and ThO_2–50%UO_2 were of diameters below 1.0 μm. The surface areas of ThO_2–30%UO_2 and ThO_2–50%UO_2 powders were 12.10 and 7.16 m^2/g, respectively. The maximum size of ThO_2 granule corresponding to −40 mesh was about 420 μm and its surface area was about 0.0014 m^2/g. The O/M ratios of the above powders were 2.218 and 2.301, respectively. The XRD powder patterns of ThO_2–30%UO_2 and ThO_2–50%UO_2 exhibited two phase structures consisting of fcc solid solution and U_3O_8. The characteristics of the starting materials of powder ThO_2 and ThO_2–UO_2 used in this study are given in Table 2. The density of the pellets of ThO_2–4%UO_2 made by using ThO_2–30%UO_2 or ThO_2–50%UO_2 powder was found to be in the range of 93–95%T.D. The ThO_2–4%UO_2 pellets sintered in Ar–8%H_2 showed a marginally higher density than those sintered in air. The densities of the pellets are given in Table 3. The XRD data of ThO_2–4%UO_2 pellets sintered either in Ar–H_2 or air showed the presence of only of fluorite phase. The O/M ratio of ThO_2–4%UO_2 pellets sintered in Ar–8%H_2 was found to be 2.00 and that for the pellets sintered in air was found to be slightly

Table 2
Characteristics of ThO_2 and (Th,U)O_2 powders.

Property	ThO_2	ThO_2–30%UO_2	ThO_2–50%UO_2
Oxygen to metal ratio	2.00	2.218	2.301
Specific surface area (m^2/g)	1.53	12.10	7.16
Total impurities (ppm)	<1200	<250	<250
Phases present	Fluorite	Fluorite and U_3O_8	Fluorite and U_3O_8
Theoretical density (g/cm^3)	10.00	10.29	10.48

Table 3
Composition, density and O/M ratio of ThO_2–4%UO_2 pellets.

Specimen details	Sintering temperature	Sintering atmosphere	Density (%T.D.)	O/M ratio
ThO_2–4%UO_2 (coating by ThO_2–50%UO_2)	1400 °C/6 h	Air	93.5	2.01
ThO_2–4%UO_2 (coating by ThO_2–30%UO_2)	1400 °C/6 h	Air	93.2	2.01
ThO_2–4%UO_2 (coating by ThO_2–50%UO_2)	1650 °C/6 h	Ar–8%H_2	94.3	2.00

Table 4
Phase, lattice parameter and O/M ratio of ThO_2–4%UO_2 sintered pellet.

Specimen details	Sintering temperature	Phases present	Lattice parameter (nm)	Mol fraction of UO_{2+x} in fluorite phase	O/M ratio
ThO_2–4%UO_2 (coating by ThO_2–50%UO_2 powder)	1400 °C/6 h, air	Fluorite	0.55912	0.0360	2.01
ThO_2–4%UO_2 (coating by ThO_2–30%UO_2 powder)	1400 °C/6 h, air	Fluorite	0.55914	0.0350	2.01
ThO_2–4%UO_2 (coating by ThO_2–50%UO_2 powder)	1650 °C/6 h, Ar–8%H_2	Fluorite	0.55923	0.0365	2.00

higher (2.01). The lattice parameters were calculated from the high angle scans (2θ = 100°–140°) by means of the Nelson-Riley extrapolation method. Table 4 gives the details of the lattice parameters and phases of the samples of the above compositions.

The as-polished microstructure of ThO_2–4%UO_2 pellet made by using ThO_2–30%UO_2 powder and sintered in air showed the existence of very fine porosities. Clustering of fine pores was observed at some places and occasionally a few linear pores were also noticed to have formed. The microstructure of ThO_2–4%UO_2 pellet made by using ThO_2–50%UO_2 powder and sintered in air showed a large number of fine pores of the size ranging 1–2 μm (Fig. 3(a)). For the pellet obtained by using ThO_2–50%UO_2 but sintered in Ar–H_2 atmosphere, the as-polished microstructure was almost identical with that sintered in air except that a few linear pores were detected. These are shown by arrows in Fig. 3(b). But the grain structure of ThO_2–4%UO_2 pellet was found to be dependent on the sintering atmosphere. The grains of the ThO_2–4%UO_2 pellet sintered in air showed a lot of variations in size. The typical microstructure is shown in Fig. 4. The grains were found to be duplex in nature. The grain size distribution is similar to 'rock in sand' structure. It was found that ThO_2 grains in the large granules (−40 mesh) are small, while the (Th,U)O_2 grains in the fine powders are large. There were packets of fine grains uniformly distributed in the matrix. The size of each of the packet is in the range of 75–100 μm. The average size of these fine grains was about 4 μm. The grain size of the matrix was 16 μm. The pore distribution was found to be non-uniform, most of the pores being located on large grained areas. The packets of fine grains were found to be dense with a very small amount of porosity.

The grain size distribution of the ThO_2–4%UO_2 pellet sintered in reducing atmosphere at 1650 °C for 6 h was more uniform. The average grain size for this sample was 45 μm. The typical microstructure is shown in Fig. 5. Another interesting feature of this sample is that a lot of fine pores of about 5 μm diameter were trapped in the grains. The SEM photographs of ThO_2–4%UO_2 pellet sintered in air and reducing atmospheres are shown in Figs. 6 and 7, respectively.

To measure the distribution of Th, U and O in the ThO_2 rich matrix, a detailed study was carried out by scanning the electron beam across the duplex structure with EPMA. An X-ray line scan result for Th M_α, U M_α and O K_α of the ThO_2–4%UO_2 pellet sintered in air is shown Fig. 8. The line scan intensities show a marginal increase in U concentration in the large grains of ThO_2–4%UO_2 pellet. The scan was also carried out on the above composition sample sintered in Ar–8%H_2 (Fig. 9). The line scan shows that the uranium concentration does not change in the pellet.

The above results are summarized below:

(1) As-polished microstructures of ThO_2–4%UO_2 pellets prepared by using either ThO_2–30%UO_2 or ThO_2–50%UO_2 powder were found to be basically the same.
(2) The microstructure of the ThO_2–4%UO_2 sintered in air showed a duplex grain structure. The grain size distribution is similar to the 'rock in sand' structure.
(3) When the above composition sample was made by sintering in Ar–8%H_2 at 1650 °C, the grains were uniform with an average grain size of 45 μm.
(4) The EPMA result for ThO_2–4%UO_2 pellets showed that the uranium concentration of the pellet sintered in air was marginally higher in the large grained areas. On the other hand, the uranium concentration of the pellet sintered in the reducing atmosphere of Ar–8%H_2 was uniform.

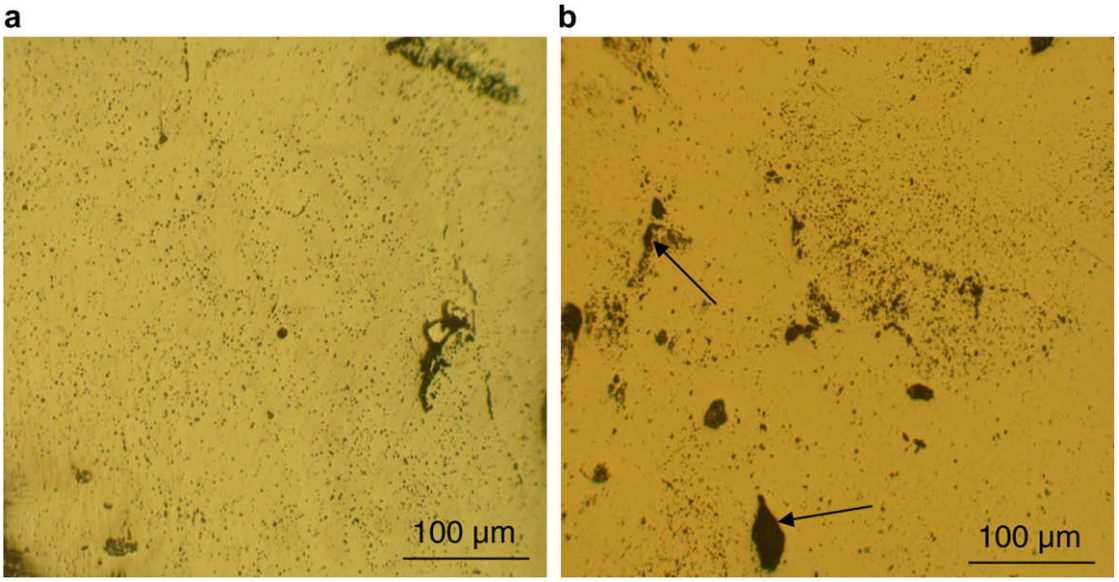

Fig. 3. As-polished microstructure of ThO_2–4%UO_2 pellet by coating with ThO_2–50%UO_2 powder; (a): Sintered in air at 1400 °C for 6 h; (b): Sintered in Ar–8%H_2 at 1650 °C for 6 h.

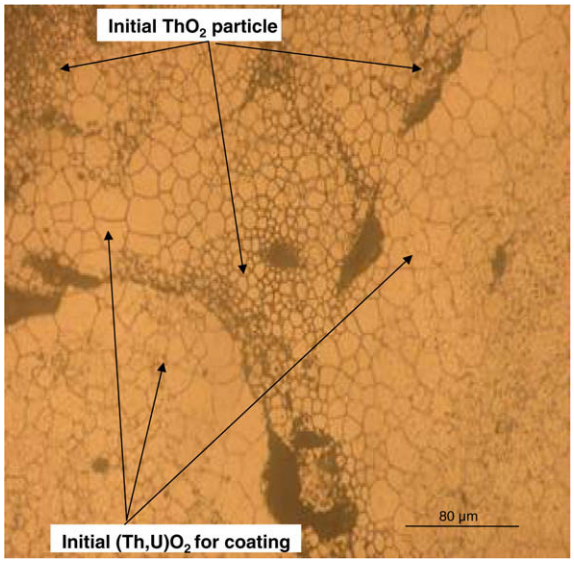

Fig. 4. Microstructure of ThO_2–4%UO_2 pellet showing duplex grain structure. Pellet: sintered in air and etched thermally.

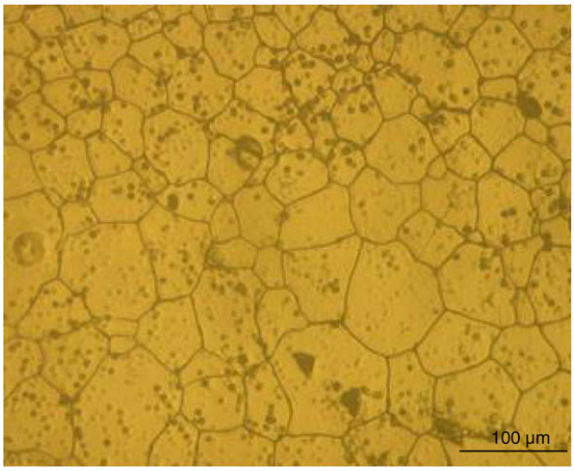

Fig. 5. Microstructure of ThO_2–4%UO_2 pellet showing uniform grain structure. Pellet: sintered in Ar–8%H_2 and etched thermally.

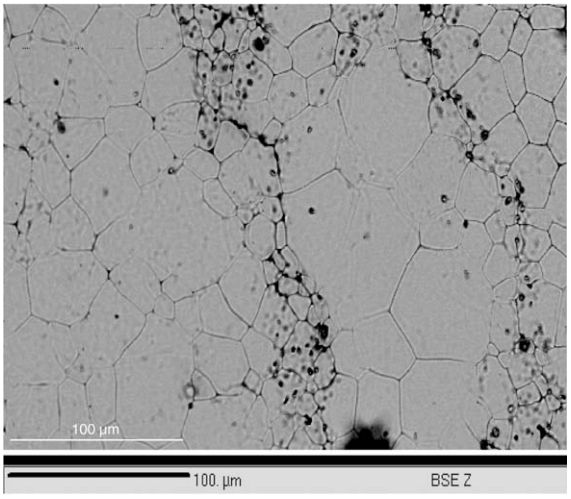

Fig. 6. SEM photograph of ThO_2–4%UO_2 pellet made by A-CAP sintered in air (1400 °C, 6 h) showing non-uniform grain structure.

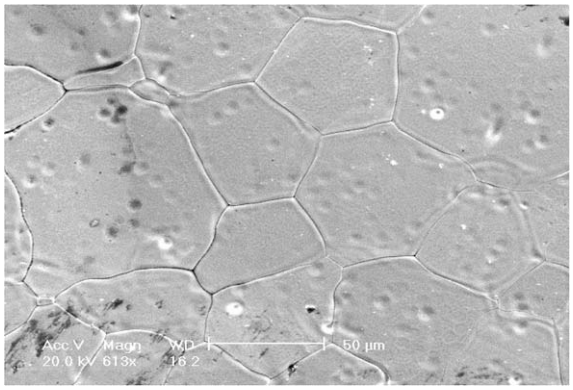

Fig. 7. SEM photograph of ThO_2–4%UO_2 pellet made by A-CAP sintered in Ar–8%H_2 (1650 °C, 6 h).

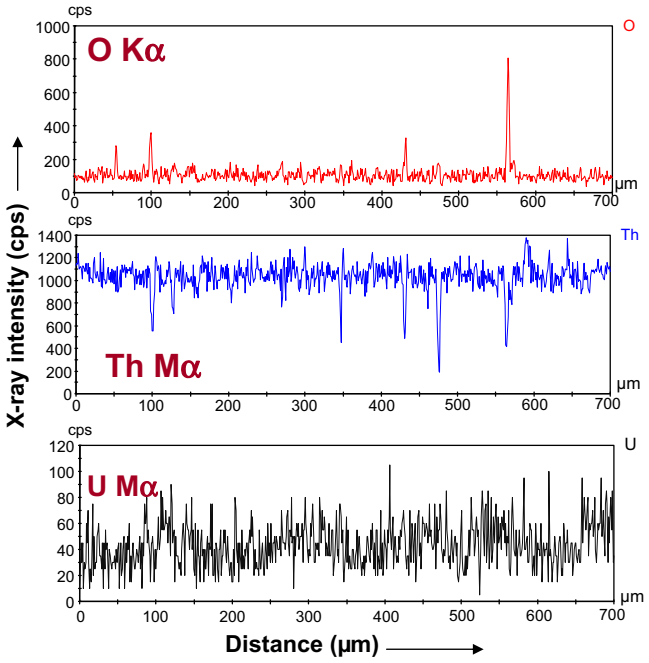

Fig. 8. X-ray line scan for Th M_α, U M_α and O K_α across the grain structure of ThO_2–4%UO_2 pellet sintered in air (1400 °C, 6 h).

5. Discussion

As mentioned in the chapter of Section 1, the CAP process was developed by BARC to replace the conventional powder metallurgy process, in which $^{233}UO_2$ is directly blended with ThO_2 powders. In this study, the CAP process was further refined in order to obtain the pellets of more improved microstructure and microhomogeneity. As shown in Section 4, the high density ThO_2–UO_2 pellets can be fabricated using the A-CAP process from the ThO_2 agglomerates and co-precipitated ThO_2–UO_2 fine powders without the addition of any dopants or sintering aids. As mentioned earlier, the choice of ThO_2–UO_2 powders as the coating material is advantageous compared to U_3O_8, since these powders give better self-shielding effect due to the presence of ThO_2. Therefore, better protection for workers is ensured while manufacturing ThO_2–UO_2 pellets using A-CAP process. With the above background in mind, we will analyze the microstructure of ThO_2–UO_2 compacts made by A-CAP process in reducing and oxidizing atmospheres.

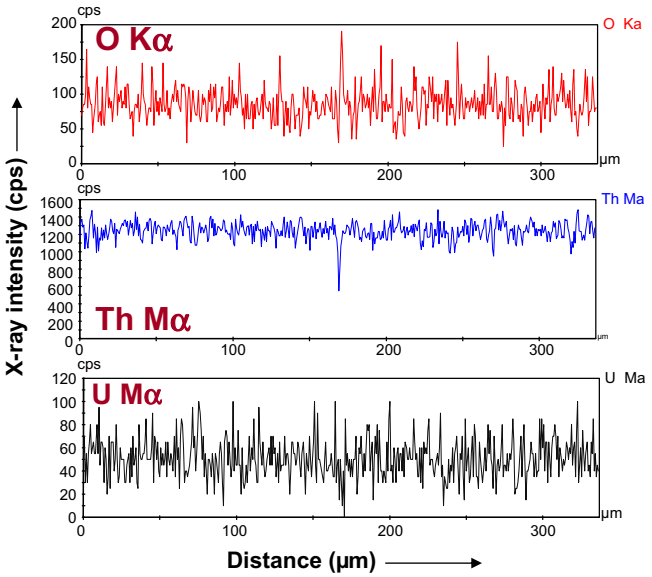

Fig. 9. X-ray line scan for Th M_α, U M_α and O K_α across the grain structure of ThO_2–4%UO_2 pellet sintered in Ar–8%H_2 (1650 °C, 6 h).

5.1. Microstructure

The microstructure of nuclear fuel plays a key role for its behaviour during irradiation. It controls the in-pile fuel behaviour like fission gas release, plasticity, in-pile creep and swelling. Moreover, the role of microstructure and crystal defects in determining the engineering properties are always acknowledged. The basic requirements for the high performance of the fuel are [2]:

(a) 'Soft pellets' – to reduce pellet clad mechanical interaction (PCMI);
(b) Large grain size – to reduce fission gas release (FGR).

The strength of the pellet at room temperature is related to grain size by the Hall–Petch relation. Accordingly, the smaller grain sized pellets will have higher strength. But at high temperature (above equicohesive temperature) the grain boundaries become weaker than grain matrix. Since the pellets of smaller grain size have wider grain boundary areas, these pellets become softer than pellets with larger grain size. Also as grain size decreases, creep rate of the fuel increases. Therefore, pellets with small grain size have higher creep rate and better plasticity at high temperatures. Therefore, these pellets will be useful to reduce the PCMI.

On the other hand, the pellets with larger grain size are beneficial to reduce the fission gas release. In developing thermal reactor fuels for high burn-up, this factor should be taken into account [2].

5.1.1. Sintering in air

As mentioned before in Section 4, the microstructure of ThO_2–4% UO_2 pellet made by CAP, sintered in air, showed a 'rock in sand' type structure [1]. In the present study, the microstructure of the same composition when sintered in air also showed a 'rock in sand' type structure but with difference. There were colonies of fine grains as observed for the CAP, but the size of the each fine grained colony was smaller. The size of the colonies obtained by the A-CAP process is in the range 75–100 μm. In the case of CAP process, the size of the fine grained colony was in range of 100–150 μm. The average size of the grains in these colonies for the pellets made by CAP and A-CAP were 2 and 4 μm, respectively. Therefore, A-CAP process yields colonies of smaller size having higher grain size compared to the CAP process. These fine grained colonies were not very dense as observed in the case of the CAP process but have some fine porosity. These colonies represent the initial ThO_2 granules, which were used for making green pellets. However, these granules now showed no boundaries between them. All the granules were fused with each other. Nowhere in the pellet, were these granules found to be delineated. This fact suggests that diffusion has occurred between ThO_2 and $(Th,U)O_2$. This is confirmed by the XRD patterns as shown in Fig. 10. Here, the XRD patterns of the staring materials, ThO_2 and ThO_2–50%UO_2 powders are shown along with that of the ThO_2–4%UO_2 sintered pellet. ThO_2–4%UO_2 pellet has shown a peak very adjacent to ThO_2. And the peaks ThO_2–50%UO_2 show a shift to (1 1 1) peak of UO_2. From the peak positions, it is clear that the solid solution has formed between ThO_2 and ThO_2–50%UO_2. The grain size of the matrix was 16 μm (Fig. 4). Compared to the CAP process, the grain size of the matrix in this study is about twice as large.

ThO_2 is the only stable oxide in the Th–O system in the condensed phase and it has very little non-stoichiometry compared to UO_2 [12–14]. Hence, the defect concentration in ThO_2 is low. Since the grain growth is a diffusion related phenomenon, it depends upon the defect concentrations such as oxygen interstitials or metal vacancies. Therefore, the grain growth is not enhanced inside the colonies. Since grain growth is diffusion controlled process, the temperature of sintering is important. Generally, diffusion processes are more prominent at temperatures >0.5T_m [15–17]. Since the temperature of the sintering used in this study was lower than 0.5T_m, this may be a factor responsible for the smaller grain sizes. These two factors resulted in developing small grains in the initial ThO_2 colonies.

The large grains observed in the coating can be explained as follows. The findings given in Section 4 show that the $(Th,U)O_2$ powders used for coating have a higher O/M ratio and larger surface area and have two phases. Such properties of surface area and O/M ratio cause to give higher density pellets after sintering. The larger surface area corresponds to higher surface energy. The driving force for sintering is the reduction in surface energy. The higher O/M ratio indicates the presence of higher concentration of oxygen interstitials. The presence of small amount of U_3O_8 in the starting powder is also assumed to have made a significant contribution to enhance sintering [1]. The amounts of U_3O_8 in the ThO_2–30%UO_2 and ThO_2–50%UO_2 powders were estimated to be 2.49 and 3.096 mol%, respectively [11]. Kutty et al. [18,19] have been

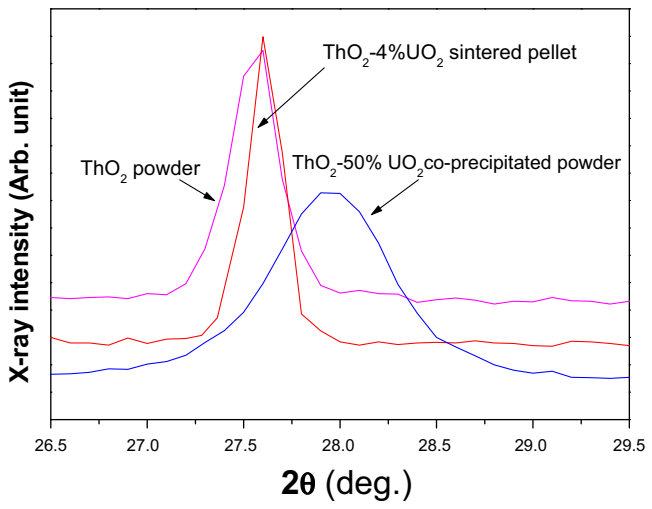

Fig. 10. XRD patterns of ThO_2 and ThO_2–50%UO_2 powders used. The XRD pattern of ThO_2–4%UO_2 sintered pellet (1400 °C in air for 6 h) is also shown in the same figure.

demonstrated that the addition of small quantities of U_3O_8 to ThO_2 enhances sintering, resulting in formation of high quality ThO_2–UO_2 pellets without the use of conventional dopants such as CaO and Nb_2O_5, which also causes to reduce the impurity level in the pellets. On increasing the temperature, the deviation from stoichiometry becomes considerably large in the ThO_2–UO_2 pellets, generating a larger number of oxygen interstitial defects. Since the diffusion coefficient of U, D^U, is proportional the square of the oxygen excess (x^2) in the lattice, sintering as well as grain growth is enhanced thus resulting in larger grains [17].

5.1.2. Sintering in Ar–8%H_2

An interesting aspect of this study was the absence of duplex microstructure when the green pellet was sintered in Ar–8%H_2. Sintering in reducing atmosphere resulted in formation of a uniform microstructure with very large grains. Hence, in this study, we have seen two different behaviours for oxidizing and reducing atmospheres. Sintering in oxidizing atmosphere resulted in duplex structure with inhomogeneity. On the other hand, sintering in reducing atmosphere resulted in good microstructure with excellent homogeneity. Let us see whether the difference in sintering temperature of 250 °C can result in such drastic change.

In the materials of the fluorite structure, the metal atoms diffuse at a much smaller rate than the non-metal atoms. The latter will therefore be rate-controlling for any diffusion controlled high temperature kinetic process. Though the predominant defects in the fluorite structure are anion defects, the less mobile cation defects, that occur at much smaller concentrations, are frequently rate determining for technologically important high temperature mass transport processes, such as grain growth, sintering, plastic deformation and creep [15,16]. Results on the diffusion of Th and U in ThO_2 have been reported by various authors [20–27], showing, however, an unusually big scatter. King [22] suggested that most of these data might be influenced by grain boundary or dislocation diffusion, and that volume diffusion proceeds at much lower rates than previously thought. The diffusion coefficient for uranium, D_U, for reactor grade ThO_2 is determined by many authors. Matzke [20] has reported the value of D_U in ThO_2 at 1400 °C and 1550 °C as 2×10^{-14} cm^2/s and 3×10^{-13} cm^2/s, respectively. Olander [26] determined the volume and grain boundary diffusion coefficients in ThO_2–UO_{2+x} mixed oxides, which were deduced from the concentration distributions established by preferential evaporation of UO_3 during air-annealing of a specimen at 1650 °C. The volume diffusion coefficient for $U_{0.1}Th_{0.9}O_{2.05}$ and $U_{0.25}Th_{0.75}O_{2.125}$ was found to be 3×10^{-14} cm^2/s and 8×10^{-13} cm^2/s, respectively.

Matzke [21] has been studied the diffusion of U in ThO_2 by conducting very extensive diffusion anneals using both polycrystals and single crystals in a broad temperature range. He reported that volume diffusion is less predominant below $0.6T_m$ for ThO_2 and was found be of the order of $\sim 10^{-18}$ cm^2/s at 1600 °C. The sintering temperature employed in this study is $\sim 0.46T_m$ and $\sim 0.53T_m$, respectively, for oxidizing and reducing atmospheres. Matzke [21] suggested that in polycrystalline ThO_2, grain boundary penetration dominates. The grain boundary diffusion coefficients for ThO_2 are 10^{-10}–10^{-9} cm^2/s at 1400–1500 °C. And at 2000 °C, the grain boundary diffusion coefficients are of the order of 10^{-7}–10^{-6} cm^2/s for the above material. Hence, it is evident that for the actinide oxides the diffusion coefficients (grain boundary) are about few orders higher than the volume diffusion. From the data for the diffusion of U and Th in ThO_2 of Matzke [21], the grain boundary diffusion coefficients are compared for 1650 °C and 1400 °C and found that the grain boundary diffusion coefficient at 1650 °C is about 100 times higher than that at 1400 °C. The study conducted at BARC on the sintering behaviour on ThO_2–UO_2 system using dilatometry has been shown that the grain boundary diffusion is the rate controlled mechanism for the initial stage of sintering. Hence, one can assume that grain boundary diffusion play an important role in sintering of the compositions covered in this study. Although sintering in oxidizing atmosphere is enhanced by the presence of defects due to the non-stoichiometry, the higher temperature used in reducing atmosphere helps in creating more intrinsic defects and helps in sintering. The higher values of diffusion coefficient (~two orders) at 1650 °C and holding at that temperature for 6 h resulted in the destruction of the duplex structure and in the improvement of the microhomogeneity.

On comparison with CAP process, the A-CAP process yields the pellets of better microstructure. In other words, coating of the ThO_2 granules with $(Th,U)O_2$ powder gives comparatively more uniform microstructure than that with U_3O_8 powder. Let us see the reason for this phenomenon. Recently Schram [28] has been constructed a data base for the oxygen potential of $Th_{1-y}U_yO_{2+x}$ solid solution. The oxygen potential of $Th_{1-y}U_yO_{2+x}$ has been measured by a number of researchers for a wide range of compositions [29–31]. It has been shown that the oxygen potential of $Th_{1-y}U_yO_{2+x}$ solid solution decreases with increase in uranium concentration (y) although it increases with the oxygen excess (x). For an O/M ratio of 2.005, the oxygen potentials for ThO_2–20%UO_2 and ThO_2–5%UO_2 at 1200 °C are −210 and −130 kJ/mol, respectively [32]. This shows that the oxygen potential of ThO_2–20%UO_2 composition at 1200 °C is about 40% lower than that of ThO_2–5%UO_2. Since ThO_2–30%UO_2 and ThO_2–50%UO_2 have a higher oxygen potential than UO_2 for the same O/M ratio, it may be a factor for its superior behaviour.

5.2. Uranium distribution

The distribution of uranium in ThO_2–4%UO_2 pellets was evaluated by EPMA (Figs. 8 and 9) for pellets sintered in oxidizing and reducing atmospheres. Both line scanning and area scanning have been carried out. For the pellet sintered in air, the line scanning of two separate colonies of fine grains revealed that uranium has diffused to the ThO_2 granules and vice versa. Semi-quantitative analysis on the large grains (uranium rich) and also on the small grains (thorium rich) has been carried out. The uranium concentration in the large grains was slightly higher than that in the smaller grains. The average uranium concentrations were 3.65 and 3.40 wt% in the large and small grains, respectively. The concentration of uranium in large grains is substantially lower than that of the starting material. This result confirms that an interdiffusion has occurred between ThO_2 and $(Th,U)O_2$ across the interface. The distribution of uranium in ThO_2–4%UO_2 pellets sintered in Ar–8%H_2 atmosphere was found to be uniform throughout the pellet. The reason of better homogeneity for the pellet sintered in reducing atmosphere may be the higher temperature (1650 °C) used for sintering. The oxygen potential of $Th_{1-y}U_yO_{2+x}$ solid solution also increases with increase in temperature for the same uranium concentration (y). These factors helped in achieving better homogeneity for ThO_2–4%UO_2 pellet when sintered in reducing atmosphere.

6. Conclusions

ThO_2–4%UO_2 pellets have been fabricated by the newly developed A-CAP route using ThO_2 and ThO_2–30%UO_2 and ThO_2–50%UO_2 powders as the starting materials. The sintered pellets were characterized in terms of microstructure and uranium distribution. The following conclusions were drawn:

(a) The microstructure of the ThO_2–4%UO_2 pellet sintered in air showed a 'rock in sand' structure with small grains in the center of granules and large grains along the periphery. However, no delineation of granules could be found.

(b) The microstructure of the above pellet sintered in Ar–8%H_2 atmosphere showed uniform grain size with large grains measuring 45 μm.
(c) The EPMA data on the sample sintered in air showed that the uranium concentration was slightly higher in the large grained areas. But for the same composition sample sintered in Ar–8%H_2 atmosphere, the uranium concentration was found to be uniform.
(d) The difference between the CAP and A-CAP processes is the amount of fine grained areas which is considerably smaller for the pellets processed by the A-CAP route.
(e) The average size of the grains in the colonies for the pellets made by CAP and A-CAP were 2 and 4 μm, respectively.

References

[1] T.R.G. Kutty, K.B. Khan, P.S. Somayajulu, A.K. Sengupta, J.P. Panakkal, Arun Kumar, H.S. Kamath, J. Nucl. Mater. 373 (2008) 299.
[2] T.R.G. Kutty, K.B. Khan, P.S. Somayajulu, A.K. Sengupta, J.P. Panakkal, Arun Kumar, H.S. Kamath, J. Nucl. Mater. 373 (2008) 309.
[3] H.S. Kamath, in: 14th Annual Conference of Indian Nuclear Society, IGCAR, Kalpakkam, 17–19th December, 2003.
[4] Nucleide 2000, Version 2, BNM-CEA/DTA/LPRI, Nuclear and Atomic Decay Data, 30th June, 2004. Available from: <www.bnm.fr>.
[5] M.S. Kazimi, M.J. Driscoll, R.G. Ballinger, K.T. Clarno, K.R. Czerwinski, P. Hejzlar, P.J. LaFond, Y. Long, J.E. Meyer, M.P. Reynard, S.P. Schultz, X. Zhao, Proliferation Resistant, Low Cost, Thoria–Urania Fuel for Light Water Reactors, Annual Report, Nuclear Engineering Department Massachusetts Institute of Technology, Cambridge, MA, 1999 (June).
[6] Philip E. MacDonald, Advanced Proliferation Resistant, Lower Cost, Uranium–Thorium Dioxide Fuels for Light Water Reactors, U.S. Department of Energy Nuclear Energy Research Initiative, NERI 99-0153, 1999.
[7] M.S. Kazimi, E.E. Pilat, M.J. Driscoll, Z. Xu, D. Wang, X. Zhao, in: International Conference on: Back-End of the Fuel Cycle: From Research to Solutions, Global 2001, Paris, France, September, 2001.
[8] M.S. Kazimi, K.R. Czerwinski, M.J. Driscoll, P. Hejzlar, J.E. Meyer, On the Use of Thorium in Light Water Reactors, MIT-NFC-0016, Nuclear Engineering Department, MIT, 1999 (April).
[9] J.R. Kennedy et al., Fuel Characterization to Support the FUTURIX-FTA Experiment, Advances for Future Nuclear Fuel Cycles, Atalante, France, 2004 (21–24th June).
[10] B.H. Lee, Y.H. Koo, D.S. Sohn, Nuclear Fuel Behaviour Modelling at High Burnup and its Experimental Support, IAEA-TECDOC-1233, International Atomic Energy Agency, Vienna, 2001. pp. 247–256.
[11] T.R.G. Kutty, K.B. Khan, P.V. Achuthan, P.S. Dhami, A. Dakshinamoorthy, P.S. Somayajulu, J.P. Panakkal, Arun Kumar, H.S. Kamath, J. Nucl. Mater., in press.
[12] M.H. Rand, in: Thorium: Physico-chemical Properties of its Compounds and Alloys, Atomic Energy Review, Special Issue No. 5, IAEA, Vienna, 1975. p. 7.
[13] J.R. Mathews, J. Chem. Soc. Faraday Trans. 83 (2) (1987) 1273.
[14] J. Belle, B. Lustman, in: Properties of UO_2, Fuel Elements Conference, Paris, TID-7546, 1958. p. 442.
[15] Hj. Matzke, in: T. Sorensen (Ed.), Non-stoichiometric Oxides, Academic Press, New York, 1981. p. 156.
[16] Hj. Matzke, Philos. Mag. 64A (1991) 1181.
[17] K.W. Lay, R.E. Carter, J. Nucl. Mater. 30 (1969) 74.
[18] T.R.G. Kutty, K.B. Khan, P.V. Hegde, A.K. Sengupta, S. Majumdar, H.S. Kamath, Sci. Sintering. 35 (2003) 125.
[19] T.R.G. Kutty, P.V. Hegde, K.B. Khan, T. Jarvis, A.K. Sengupta, S. Majumdar, H.S. Kamath, J. Nucl. Mater. 335 (2004) 462.
[20] Hj. Matzke, J. Nucl. Mater. 21 (1967) 190.
[21] Hj. Matzke, J. Physique colloq. C-7 (1976) 452.
[22] D.A. King, J. Nucl. Mater. 38 (1971) 347.
[23] H. Furuya, J. Nucl. Mater. 26 (1968) 123.
[24] R.J. Hawkins, C.B. Alcock, J. Nucl. Mater. 26 (1967) 112.
[25] Ken, Ando, Y. Ideda, S. Morita, R. Watanabe, J. Nucl. Mater. 136 (1985) 186.
[26] D.R. Olander, J. Nucl. Mater. 144 (1987) 105.
[27] Hj. Matzke, J. Chem. Soc. Faraday Trans. 86 (1990) 1243.
[28] R.P.C. Schram, J. Nucl. Mater. 344 (2005) 223.
[29] M. Ugajin, J. Nucl. Mater. 110 (1982) 142.
[30] T.B. Lindemer, T.M. Besmann, J. Nucl. Mater. 130 (1985) 473.
[31] T. Matsui, K. Naito, J. Nucl. Mater. 132 (1985) 212.
[32] K. Bakker, E.H.P. Cordfunke, R.J.M. Konings, R.P.C. Schram, J. Nucl. Mater. 250 (1997) 1.